Title
T + 2 AMD T = 3 ANALOGUE STATES, 28 < A < 40

Authors
Hardy, J.C.
Brunnader, H.
Cerny, Joseph.

Publication Date
1969-06-01

Submitted to Physical Review

UCRL-18942
Preprint

T = 2 AND T = 3 ANALOGUE STATES, $28 \leq A \leq 40$

J. C. Hardy, H. Brunnader, and Joseph Cerny

June 1969

AEC Contract No. W-7405-eng-48

LAWRENCE RADIATION LABORATORY
UNIVERSITY of CALIFORNIA BERKELEY

UCRL-18942

DISCLAIMER

T = 2 AND T = 3 ANALOGUE STATES, $28 \leq A \leq 40$*

J. C. Hardy, H. Brunnader† and Joseph Cerny

Lawrence Radiation Laboratory and
Department of Chemistry, University of
California, Berkeley, California 94720

June 1969

ABSTRACT

The simultaneous observation of (p,t) and (p,^{3}He) reactions has led to the location and identification of the lowest-energy (0^+) T = 2 states in ^{28}Al, ^{28}Si, ^{32}P, ^{32}S, ^{36}Cl, ^{36}Ar, ^{40}K and ^{40}Ca, as well as the (0^+) T = 3 states in ^{38}Cl and ^{38}Ar. The energies of these states are used to predict the masses of six neutron-deficient nuclei: ^{28}S, ^{32}Ar, ^{36}Ca, ^{38}Sc, ^{38}Ti and ^{40}Ti. In addition, the (p,t) cross section for production of each analogue state relative to the cross section for producing the ground state in the same nucleus is compared with calculations which assume a simple shell model. Good agreement is obtained.

*This work was performed under the auspices of the U. S. Atomic Energy Commission.

†Present address: Department of Chemistry, McMaster University, Hamilton, Ontario, Canada.

I. INTRODUCTION

The advent of new experimental techniques for measuring the masses of neutron-deficient nuclei has led to recent interest in investigating the limits of stability in the lighter nuclides. As an aid to such measurements, accurate mass predictions are of great value, and for this purpose the isobaric-multiplet mass equation (IMME) is frequently used:

$$M(A,T,T_z) = a(A,T) + b(A,T)\, T_z + c(A,T)\, T_z^2 \quad . \tag{1}$$

This equation has the advantage that it is easy to apply and is apparently reliable[1] — more reliable than might be indicated by the first-order perturbation theory used in its derivation.[2] However, use of the equation for predicting the mass of a particular state requires knowledge of the masses of three other members of the same multiplet since the coefficients a, b and c must be experimentally determined for each value of A and T. The masses of all $T_z = +2$ ($A = 4n$) nuclei are known to better than ±10 keV in the region $28 \leqslant A \leqslant 40$ and consequently, for each value of A, measurement of the excitation energies of T = 2 analogue states in two other isobars permits use of the IMME for relatively accurate predictions of other members of the multiplet. Similarly, the measurement of two T = 3 states in mass-38 combined with the less accurately known mass (±150 keV) of ^{38}S yields rough predictions for that multiplet.

We report here the location and identification of the lowest-energy (0^+) T = 2 states in ^{28}Al, ^{28}Si, ^{32}P, ^{32}S, ^{36}Cl, ^{36}Ar, ^{40}K and ^{40}Ca, as well as the T = 3 states in ^{38}Cl and ^{38}Ar. The method used was to simultaneously

observe the (p,t) and (p,^{3}He) reactions. If the target nucleus has isospin T_i and the reactions produce analogue final states with $T_f = T_i + 1$, then their angular distributions will have the same shape and the ratio of their differential cross sections will be given by:

$$R \equiv \frac{\frac{d\sigma}{d\Omega}(p,t)}{\frac{d\sigma}{d\Omega}(p,{}^3\mathrm{He})} \frac{k_t}{k_{^3\mathrm{He}}} \cdot \frac{2}{2T_f - 1} \quad . \tag{2}$$

The approximations leading to the derivation of Eq. (2) have recently been discussed[3] and their validity established. The properties embodied in the equation provide an unambiguous experimental method for identifying high isospin analogue states.

Using the experimental data, masses are predicted with the IMME for ^{28}S, ^{32}Ar, ^{36}Ca, ^{38}Sc, ^{38}Ti and ^{40}Ti. These results are compared with those obtained by Kelson and Garvey.[4] In addition, the relative intensities of the analogue state transitions are compared with calculations which assume simple shell-model configurations.

II. EXPERIMENTAL PROCEDURE

This series of measurements was carried out using the 45 MeV proton beam from the Berkeley 88-inch cyclotron. The beam was magnetically analyzed to give an energy resolution of $\sim 0.14\%$, and was focused to a spot 2 mm × 1.5 mm at the target position in the center of a 50-cm scattering chamber. The exact position and direction of the beam was determined by observing luminous foils located at the target position and 70 cm downstream. The beam current ranged from 50 nA to 1.0 μA depending on target thickness and scattering angle; it was monitored with a Faraday cup connected to an integrating electrometer. The beam energy was inferred from measuring its range in a series of aluminum foils which were contained in five remotely controlled wheels.

A detailed diagram of the scattering chamber, gas target and gas-handling apparatus is shown in Fig. 1. The gas cell consisted of a stainless steel cylindrical frame 6.35 cm in diameter and 2.22 cm high surrounded by a 315° continuous window of 2.5 μ Havar foil.[5] An expanded view of the frame is shown in the insert to the figure. The gas cell was designed for minimum volume (47 cm^3) in order to permit the efficient recovery of separated-isotope gases. To use solid targets, the gas cell was removed and a set of targets was mounted in a holder which could then be raised and lowered remotely, thus permitting bombardment of any selected target.

Reaction products were detected using two independent counter telescopes mounted 10° out of the horizontal plane on opposite sides of the beam. The solid angle subtended by each telescope was $\sim 5 \times 10^{-5}$ sr, with an angular resolution of 0.26°. For solid targets, a tantalum collimator 5 mm high by

2 mm wide was mounted 48 cm from the target, while for gas targets an additional collimator with the same width as the first was mounted 36 cm ahead of it. Each telescope consisted of three detectors, a 150 μ phosphorus-diffused silicon transmission counter (ΔE) operated in coincidence with a 3 mm lithium-drifted silicon E counter, and a 500 μ lithium-drifted silicon E-reject counter operated in anti-coincidence with the first two to eliminate long-range protons and deuterons.

A schematic diagram of the electronics used is shown in Fig. 2. The signals from each telescope were fed into a Goulding-Landis particle identifier[6] which produced an output signal characteristic of the particle type. This signal was used to route the total-energy signal (E + ΔE) into one of the 1024-channel segments of a 4096-channel analyzer permitting simultaneous accumulation of α-particles, ^{3}He-particles, tritons, and those particles slightly less ionizing than the selected tritons. The first and last groups were taken to check that no ^{3}He or triton events were lost.

III. EXPERIMENTAL RESULTS

The excitation energies of observed states were determined by analyzing the data with the computer program LORNA.[7] This program corrects the energies of incoming and outgoing particles for kinematic effects and absorber losses, then determines the energies of unknown peaks using an energy scale established from a least-squares fit to peaks whose Q-values are known. For the experiments described here, contaminants were already present or introduced in the targets to provide calibration. The most useful calibration reactions were $^{12}C(p,t)^{10}C$ and $^{12}C(p,^3He)^{10}B$: the masses of the ^{10}C ground and first excited states were taken from recent measurements[8] while values for the levels of ^{10}B were taken from Ajzenberg-Selove and Lauritzen.[9]

A. $^{30}Si(p,t)^{28}Si$ and $^{30}Si(p,^3He)^{28}Al$, T = 2 States

Triton and ^3He spectra from a 400 $\mu g/cm^2$ self-supporting silicon target are shown in Fig. 3; they were obtained at $\theta_{lab} = 18.0°$ for 2150 μc. The isotopic enrichment of the target was 89.12% in ^{30}Si with 10.16% ^{28}Si and 0.72% ^{29}Si. Spectra were recorded for seven angles ranging from $\theta_{lab} = 14.1°$ to $\theta_{lab} = 36.2°$.

The energy scale was determined using peaks produced from reactions on ^{12}C, ^{16}O and ^{28}Si as well as those known states produced in ^{28}Si and ^{28}Al; all have been indicated in the figure. Rough Coulomb-energy calculations predict the excitation energy of the T = 2 state to be 15.3 MeV in ^{28}Si and 6.1 MeV in ^{28}Al. The states marked T = 2 in Fig. 3 are consistent with these expectations, and the angular distribution of the corresponding tritons and

^{3}He-particles are shown at the top of the Fig. 4. The ^{3}He data points have been multipled by $\frac{2}{3} \cdot \frac{k_t}{k_{^3He}}$ (=0.62) so that the applicability of Eq. (2) can be tested directly. To the accuracy of the approximations used to derive that equation, the shapes and magnitudes of the distributions as they appear in the figure are the same, and consequently the levels are established as T = 2 analogues. Also shown in Fig. 4 are the characteristic L = 0 and L = 2 angular distributions of the (p,t) reaction leading to the ground (0^+) and first excited (2^+) state of ^{28}Si. A simple comparison shows that the angular momentum transfer to the analogue states is also L = 0 and this identifies them as the 0^+ analogues of the ^{28}Mg ground state.

Further verification of the assigned L-transfer was provided by calculations using the distorted wave Born approximation (DWBA). The calculations were performed using the program DWUCK[10] with the optical-model parameters[11,12] given in Table I, and the results are shown normalized to the experimental data in Fig. 4. The agreement is good.

A summary of results on these mass-28 analogue states is shown in Table II. We have previously reported our measured excitation energies in a letter[13] devoted to the decay of the T = 2 state in ^{28}Si. Subsequently, by searching in the indicated energy region, the analogue state in ^{28}Si was observed as a resonance in the ^{24}Mg(α,α)^{24}Mg reaction[14,15] and the ^{24}Mg(α,γ)^{28}Si* reaction,[14,16] and also as a final state in the ^{26}Mg(^{3}He,n)^{28}Si reaction.[17] The best value from these other measurements[18] is also shown in Table II. It agrees well with our original value.

B. $^{34}S(p,t)^{32}S$ and $^{34}S(p,^3He)^{32}P$, T = 2 States

A self-supporting cadmium sulfide target approximately 100 $\mu g/cm^2$ thick was used for this experiment. The sulfur component was enriched to 67.92% in ^{34}S with 31.55% ^{32}S, 0.44% ^{33}S and 0.09% ^{36}S. Because the thin target could only withstand small beam intensities, the counting rates were low and consequently spectra were recorded at only four angles ranging from $\theta_{lab} = 20.5°$ to $\theta_{lab} = 31.5°$. Triton and ^3He spectra obtained at $\theta_{lab} = 22.30$ for 6380 μc are shown in Fig. 5. A natural cadmium sulfide target was also bombarded and spectra taken at the same angle in order to identify those states in ^{30}S and ^{30}P which were produced from the enriched target. These states have been marked in the figure and were used, together with the other marked states, to establish the energy calibration.

The states identified in the figure as being T = 2 are at excitation energies consistent with predictions based on Coulomb energy calculations, and the ratio of differential cross sections for the reactions populating these states has an average value for the four observed angels of 0.66 ± 0.06. This agrees well with the value of 0.60 calculated from Eq. (2), thus establishing the T = 2 character of the states. In addition, their energy and the fact that their observed angular distributions are consistent with L = 0 transfer identify the states as 0^+ analogues to the ground state of ^{32}Si.

These results are summarized in Table II. The excitation energies shown there have appeared prior to this publication in a review article[1] and, as with mass-28, the energy of the T = 2 state in ^{32}S was subsequently remeasured using a resonance reaction;[19] this result also appears in the Table.

C. $^{38}Ar(p,t)^{36}Ar$ and $^{38}Ar(p,^{3}He)^{36}Cl$, T = 2 States

Spectra of tritons and ^{3}He-particles from an ^{38}Ar-enriched target are shown in Fig. 6; they were recorded at 22.3° for 7562 μc. The isotopic composition of the gas target was 23.3% ^{36}Ar, 50.8% ^{38}Ar and 25.9% ^{40}Ar. Altogether, spectra were obtained for fifteen angles from $\theta_{lab} = 11.7°$ to $\theta_{lab} = 50.7°$

Under identical running conditions, ^{36}Ar and ^{40}Ar targets were bombarded in order to identify peaks produced from these isotopes. Following this identification, the energy calibration of the original spectra could be accomplished by means of known states in mass-34,[20,21] mass-36 and mass-38;[21] all have been marked with their excitation energy (unbracketed) and isotopic mass in the figure. The states labelled T = 2 have measured energies which agree with rough Coulomb-energy predictions for the analogue states and their corresponding triton and ^{3}He angular distributions are shown at the top of Fig. 7. The similarity of the shapes and magnitudes of the distributions as they appear in the figure show that the conditions of Eq. (2) are satisfied, and identifies the states as T = 2 analogues. By comparison with known L = 0 and L = 2 transitions (also shown in Fig. 7) and with DWBA calculations (solid curves in the figure) the angular-momentum transfer for transitions to their analogue states is determined to be L = 0. Thus, the states must be the 0^{+} analogues to the ground state of ^{36}S. Their measured energies are listed in Table II. There has been a recent measurement[22] of a state in ^{36}Cl proposed as the T = 2 analogue state; it is also listed in Table II and agrees with our value.

D. $^{40}Ar(p,t)^{38}Ar$ and $^{40}Ar(p,^{3}He)^{38}Cl$; T = 3 States

Pure natural argon, which is 99.6% ^{40}Ar, was used to obtain triton and ^{3}He angular distribution data while energy calibration resulted from the use of an argon-methane (80% - 20% respectively) mixture. In Fig. 8 are shown sample spectra taken, using the latter target, at 26.8° for 12,553 μc. In all, spectra were recorded at fifteen angles between θ_{lab} = 11.7° and θ_{lab} = 50.7°.

As in the cases already described, the states labelled T = 3 in Fig. 8 have appropriate excitation energies. Their points have been multiplied by $\frac{2}{5}\frac{k_t}{k_{^3He}}$ (= 0.35). Evidently the requirements of Eq. (2) are satisfied and the states are identified as T = 3 analogues. It should be pointed out that the error bars which appear on the data points in Fig. 9, like those in other figures, are based purely on counting statistics and do not take account of the uncertainties in background subtraction. In this case these uncertainties are not negligable for the (p,t) reaction and probably account for the discrepancies between (p,t) and (p,^{3}He) distributions near 45°.

The comparison with known transitions and DWBA calculations afforded by Fig. 9 determine the T = 3 states to be 0^{+}, and establish them as analogues to the ^{38}S ground state. Their measured energies are listed in Table II.

E. $^{42}Ca(p,t)^{40}Ca$ and $^{42}Ca(p,^{3}He)^{40}K$; T = 2 States

Since the T = 2 states have already been identified[1] in ^{40}Ca and ^{40}K, no attempt was made here to obtain detailed angular distributions; our purpose was to reduce the uncertainty of the measured excitation energies. The calcium target used was enriched to 94.42% ^{42}Ca with 4.96% ^{40}Ca, 0.06 % ^{43}Ca,

0.56% ^{44}Ca and only trace amounts of ^{46}Ca and ^{48}Ca. A series of four angles from $\theta_{lab} = 18.0°$ to $\theta_{lab} = 31.5°$ was measured, the pair of spectra obtained at $\theta_{lab} = 26.8°$ for 3554 μc being shown in Fig. 10.

The excitation energies of the analogue states were determined from an energy scale established by the states labeled in the figure. Their angular distributions are consistent with zero angular-momentum transfer and the ratio of their magnitudes agrees with the requirements of Eq. (2). The states are thus confirmed as being 0^+ analogues to the ground state of ^{40}Ar. Their measured excitation energies appear in Table II.

IV. DISCUSSION

Table III summarizes the data obtained from these experiments on the cross-section ratios for the production of analogue states which have $T_f = T_i + 1$. The third column contains the experimental data for $\frac{d\sigma}{d\Omega}(p,t)/\frac{d\sigma}{d\Omega}(p,{}^3He)$ while the fourth column gives the results of calculations using Eq. (2); in all cases, agreement is within the limits of experimental uncertainty. The recent discussion[3] of the validity of Eq. (2) includes these and other results covering the range $16 \leq A \leq 42$ and $1 \leq T_f \leq 3$. The agreement with calculation is uniformly excellent.

It is also of interest to investigate the strength of the (p,t) reaction leading to a particular analogue state (with $T_> = |T_z| + 2$) compared to the strength of the reaction to another state in the same final nucleus; for simplicity we have chosen the ground state (which has $T_< = |T_z|$). The comparison between the experimental results and calculations which assume simple shell-model configurations is given in Table IV. In addition to the configurations which are listed in the Table for the analogue states, the calculations assumed the simplest possible configurations for the ground state of the targets and final nuclei; for example, the ground state of ^{30}Si is assumed to be $(2s_{1/2})^2_{01}$ while that of ^{40}Ar is $[(1d_{3/2})^{-2}_{01}(1f_{7/2})^2_{01}]_{02}$.

It must be emphasized that, unlike the results in Table III, the present calculations will depend considerably upon details of the DWBA computations since the Q-values are significantly different for the two final states produced from each target. Unfortunately, optical-model parameters are not available for tritons at our experimental energies ($19 \leq E_t \leq 39$ MeV). The triton parameters listed in Table I were obtained from elastic scattering

at 12 MeV, and although they provide reasonable fits to our experimental data (Figs. 4, 7 and 9), there is no guarantee that they will also provide reliable values for the calculated cross-section ratios. Consequently, several parameter-sets were used on the calculations for Table IV. These included, in addition to the sets in Table I, parameters obtained from a re-analysis of the same 12 MeV elastic-scattering data[23] and also a set which attempted to take account of the dependence of V and W upon the triton energy.[24] Each provided adequate agreement with the shapes of the experimental angular distributions, but the calculated cross-section ratios depended significantly upon the set being used. The ranges of values obtained for each reaction are listed in the third column of Table IV. Good agreement is found between experiment and theory with the possible exception of the reaction $^{34}S(p,t)^{32}S$. For this case the most probable simple configuration for the analogue state requires $(2s_{1/2})^2$ pick-up to that state, but $(1d_{3/2})^2$ to the ground state. Here the disagreement with experiment indicates that the transfer involves more complex configurations possibly including $(1d_{5/2})^2$ pick-up to the analogue state.

Obviously, the simple configurations assumed here for the wave functions of all the states involved are unrealistic; however, the good overall agreement in Table IV cannot be ignored since the (p,t) reaction is generally very sensitive to details of the assumed wave functions. In addition, three more cases of similar agreement are known[1,25] and together with the present data they span the region $20 \leq A \leq 52$. Presumably these results reflect the fact that the parentage of both the ground and analogue states are reasonably simple even if the wave functions themselves are not.

This indication is similar to the more definite results recently obtained[3] for certain states in the same mass region with $T_f = T_i$.

Using the IMME (Eq. (1)) and measured energies from Table II, masses can be predicted for a number of neutron-deficient nuclei which are as yet unobserved. The results are given in Table V together with the predictions of Kelson and Garvey.[4] Both sets of predictions agree throughout.

The method followed in this experiment has been used previously by us to identify analogue states with $T \leqslant 2$ (where $T > |T_z|$). It has been restricted to these low values of T by the fact that the ratio in Eq. (2) is inversely proportional to $(2T_f - 1)$, and for analogue states with higher values of T it was anticipated that the (p,t) cross section could be prohibitively small. The observation and firm identification of $T = 3$ states in mass-38 indicate that higher-isospin states can in fact be adequately studied. Consequently, it appears that such investigations as these can be extended to heavier nuclei, particularly those in the $(1f_{7/2})$-shell.

V. ACKNOWLEDGMENT

One of us (J. C. H.) gratefully acknowledges a fellowship from the Miller Institute for Basic Research in Science.

REFERENCES

1. J. Cerny, Ann. Rev. Nucl. Sci. 18, 27 (1968).
2. J. Jänecke, Nucl. Phys. A128, 632 (1969).
3. J. C. Hardy, H. Brunnader and J. Cerny, Phys. Rev. Letters 22, 1439 (1969).
4. I. Kelson and G. T. Garvey, Phys. Letters 23, 689 (1966).
5. Havar foil is manufactured by the Metals Division, Hamilton Watch Company, Lancaster, Pa.
6. F. S. Goulding, D. A. Landis, J. Cerny and R. H. Pehl, Nucl. Instr. and Methods 31, 1 (1964).
7. The program LORNA was written by C. C. Maples to whom we are grateful for making it available.
8. H. Brunnader, J. C. Hardy and J. Cerny, Phys. Rev. 174, 1247 (1968); R. A. Paddock, S. M. Austin, W. Benenson, I. D. Proctor and F. St. Ament, Phys. Rev. (in press).
9. F. Ajzenberg-Selove and T. Lauritzen, Nucl. Phys. A114, 1 (1968).
10. The program DWUCK was written by D. Kuntz, and modified for two-nucleon transfer reactions following the "zero-range interaction" approximation [see N. K. Glendenning, Phys. Rev. 137, B102 (1965)] by us.
11. Average parameters taken from fits to 40 MeV elastic proton scattering by M. P. Fricke, E. E. Gross, B. J. Morton and A. Zucker, Phys. Rev. 156, 1207 (1967).
12. R. N. Glover and A. D. W. Jones, Nucl. Phys. 81, 268 (1966).
13. R. L. McGrath, J. C. Hardy and J. Cerny, Phys. Letters 27B, 443 (1968).
14. K. A. Snover, D. W. Heikkinen, F. Riess, H. M. Kuan and S. S. Hanna, Phys. Rev. Letters 22, 239 (1969).

14. K. A. Snover, D. W. Heikkinen, F. Riess, H. M. Kuan and S. S. Hanna, Phys. Rev. Letters 22, 239 (1969).

15. G. H. Lentz, M. P. Etten and D. Wilkins, Bull. Am. Phys. Soc. 14, 548 (1969) — this replaces an earlier erroneous report by G. H. Lentz and D. Bernard, Bull. Am. Phys. Soc. 13, 673 (1968).

16. T. T. Thwaites, P. Kupferman and S. Slack, Bull. Am. Phys. Soc. 14, 566 (1969).

17. W. Bohne, H. Fuchs, K. Grabisch, M. Hagen, H. Homeyer, U. Janetzki, H. Lettau, K. H. Maier, H. Morgenstern, P. Pietrzki, G. Röschert and J. A. Scheer, (to be published).

18. The actual excitation energies measured (in MeV) are 15.221 ± 0.005,[15] 15.196 ± 0.010,[16] 15.216[17] (no quoted error, but presumably less than ± 0.010), and 15.27 ± 0.05.[18] With the exception of the second, these values are consistent with one another. The result in Ref. 15 is the one quoted in Table II since it is the most accurate, and the only one which has actually been published.

19. D. W. Heikkinen, H. M. Kuan, K. A. Snover, F. Riess, and S. S. Hanna, Bull. Am. Phys. Soc. 13, 884 (1968); although the 11.984 MeV state is the only observed resonance in the energy region of the T = 2 state, its identification from observed γ-rays is not conclusive (private communication from D. W. Heikkinen).

20. H. Brunnader, J. C. Hardy and J. Cerny, Nucl. Phys., (to be published).

21. P. M. Endt and C. van der Leun, Nucl. Phys. A105, 1 (1967).

22. L. Broman, C. M. Fou and B. Rosner, Nucl. Phys. A112, 195 (1968).

23. Private communication from R. N. Glover.

24. S. W. Cosper, H. Brunnader, J. Cerny, and R. L. McGrath, Phys. Letters 25B, 324 (1967).

25. I. S. Towner and J. C. Hardy, Direct Two-Nucleon Transfer Reactions and their Interpretation in Terms of the Nuclear Shell Model, (Report 19/68, Nuclear Physics Laboratory, Oxford).

Table I. Optical model parameters[a] used in DWBA calculations.

Particle	V_o	W_o	W_D	V_s	r_o	r'_o	r_s	a	a'	a_s	Ref.
proton	45.0	5.7	1.8	6.04	1.16	1.37	1.064	0.75	0.63	0.738	b
triton + ^{28}Si	147.1	54.1	-	-	1.40	1.40	-	0.61	0.61	-	c
Triton + $^{36}Ar, ^{38}Ar$	143.3	53.3	-	-	1.40	1.40	-	0.59	0.59	-	c

[a]The form of the potential and the notation followed in this table are identical to those used in Reference 11.

[b]Reference 11.

[c]Reference 12.

Table II. Summary of experimental results for high T states.

Nucleus	Analogue State $J^{\pi};T$	Excitation Energy This work (MeV ± keV)	Other work (MeV ± keV)	Average (MeV ± keV)
^{28}Al	0^+; 2	5.983 ± 25	---	[5.983 ± 25]
^{28}Si	0^+; 2	15.206 ± 25	15.221 ± 5 [a]	15.221 ± 5
^{32}P	0^+; 2	5.071 ± 40	---	[5.071 ± 40]
^{32}S	0^+; 2	12.034 ± 40	11.984 ± 4 [b]	11.984 ± 4
^{36}Cl	0^+; 2	4.295 ± 30	4.333 ± 25 [c]	4.316 ± 19
^{36}Ar	0^+; 2	10.858 ± 35	---	[10.858 ± 35]
^{38}Cl	0^+; 3	8.216 ± 25	---	[8.216 ± 25]
^{38}Ar	0^+; 3	18.784 ± 30	---	[18.784 ± 30]
^{40}K	0^+; 2	4.375 ± 25	4.370 ± 70 [d]	4.374 ± 24
^{40}Ca	0^+; 2	11.978 ± 25	11.970 ± 65 [d]	11.977 ± 23

[a] References 14-17.

[b] Reference 19.

[c] Reference 22.

[d] Reference 1.

Table III. Experimental and calculated relative cross-sections $\frac{d\sigma}{d\Omega}(p,t)/\frac{d\sigma}{d\Omega}(p,{}^3He)$ for states with $T_f = T_i + 1$.

States		$J^\pi;T$	R(exp)	R(calc)
^{28}Si	15.221 MeV	$0^+;2$	0.54 ± 0.10	0.60
^{28}Al	5.983 MeV			
^{32}S	11.984 MeV	$0^+;2$	0.66 ± 0.06	0.60
^{32}P	5.071 MeV			
^{36}Ar	10.858 MeV	$0^+;2$	0.62 ± 0.07	0.60
^{36}Cl	4.316 MeV			
^{38}Ar	18.784 MeV	$0^+;3$	0.36 ± 0.04	0.35
^{38}Cl	8.216 MeV			
^{40}Ca	11.977 MeV	$0^+;2$	0.60 ± 0.05	0.60
^{40}K	4.374 MeV			

Table IV. Experimental and calculated ratios for the production of the $T_> = |T_z| + 2$ analogue state relative to the $T_< = |T_z|$ ground state for several (p,t) reactions.

Reaction	Assumed analogue-state configuration	$\frac{d\sigma}{d\Omega}(T_>)/\frac{d\sigma}{d\Omega}(T_<)$ Calculated[a]	Experimental
$^{30}Si(p,t)^{28}Si$	$[(1d_{5/2})^{-2}_{01}(2s_{1/2})^{2}_{01}]_{02}$	0.15 - 0.45	0.15 ± 0.02
$^{34}S(p,t)^{32}S$	$[(2s_{1/2})^{-2}_{01}(1d_{3/2})^{2}_{01}]_{02}$	0.65 - 2.0	0.19 ± 0.04
	$[(1d_{5/2})^{-2}_{01}(1d_{3/2})^{2}_{01}]_{02}$	0.21 - 1.0	
$^{38}Ar(p,t)^{36}Ar$	$(1d_{3/2})^{4}_{02}$	0.13 - 0.40	0.19 ± 0.02
$^{40}Ar(p,t)^{38}Ar$	$[(1d_{3/2})^{-4}_{02}(1f_{7/2})^{2}_{01}]_{03}$	0.05 - 0.15	0.07 ± 0.02
$^{42}Ca(p,t)^{40}Ca$	$[(1d_{3/2})^{-2}_{01}(1f_{7/2})^{2}_{01}]_{02}$	0.13 - 0.30	0.18 ± 0.03

[a]For each reaction, a range of values is shown encompassing the results of DWBA calculations with a variety of plausible optical-model triton parameters[12,23,24] (see discussion in text).

Table V. Predicted mass excesses of unmeasured neutron deficient nuclei

Nucleus	T_z	Estimated mass from IMME (MeV ± keV)	Kelson-Garvey[a] mass predictions (MeV)
^{28}S	-2	4.31 ± 200	4.44
^{32}Ar	-2	-2.59 ± 320	-2.28
^{36}Ca	-2	-6.58 ± 210	-6.48
^{38}Sc	-2	-4.55 ± 1020[b]	-4.70
^{38}Ti	-3	11.08 ± 1680	10.82
^{40}Ti	-2	-9.07 ± 265	-9.07

[a]Reference 4.

[b]This prediction is based on the assumption that the T = 3 state in ^{38}Sc lies at the same excitation as its analogue in ^{38}Cl.

FIGURE CAPTIONS

Fig. 1. Diagram of the scattering chamber, gas target and gas handling apparatus.

Fig. 2. Schematic diagram of the electronic apparatus used in conjunction with the counter telescopes: only system 1 is shown in its entirety, system 2 being similar.

Fig. 3. Energy spectra of the reactions $^{30}Si(p,t)^{28}Si$ and $^{30}Si(p,^{3}He)^{28}Al$.

Fig. 4. Angular distributions for the reactions $^{30}Si(p,t)^{28}Si$ and $^{30}Si(p,^{3}He)^{28}Al$ leading to selected final states. Note that the $(p,^{3}He)$ data for the T = 2 state has been multiplied by 0.62 as suggested by Eq. (2). The solid curves correspond to DWBA calculations for L = 0 and L = 2 transfer using the parameters given in Table I

Fig. 5. Energy spectra of the reactions $^{34}S(p,t)^{32}S$ and $^{34}S(p,^{3}He)^{32}P$.

Fig. 6. Energy spectra of the reactions $^{38}Ar(p,t)^{36}Ar$ and $^{38}Ar(p,^{3}He)^{36}Cl$. The excitations shown bracketed were determined in this work, the calibration having been established from the other marked states.

Fig. 7. Angular distributions of the reaction $^{38}Ar(p,t)^{36}Ar$ and $^{38}Ar(p,^{3}He)^{36}Cl$ leading to selected final states. The $(p,^{3}He)$ data for the T = 2 state has been multiplied by 0.60 as suggested by Eq. (2). The solid curves correspond to DWBA calculations for L = 0 and L = 2 transfer using the parameters given in Table I.

Fig. 8. Energy spectra of the reactions $^{40}Ar(p,t)^{38}Ar$ and $^{40}Ar(p,^{3}He)^{38}Cl$. The states shown bracketed were determined in this work, the calibration having been established using the other marked states.

Fig. 9. Angular distributions of the reactions $^{40}Ar(p,t)^{38}Ar$ and $^{40}Ar(p,^{3}He)^{38}Cl$ leading to selected final states. The $(p,^{3}He)$ data has been multipled by 0.350 as suggested by Eq. (2). The solid curves correspond to DWBA calculations for L = 0 and L = 2 transfer using the parameters given in Table I.

Fig. 10. Energy spectra of the reactions $^{42}Ca(p,t)^{40}Ca$ and $^{42}Ca(p,^{3}He)^{40}K$.

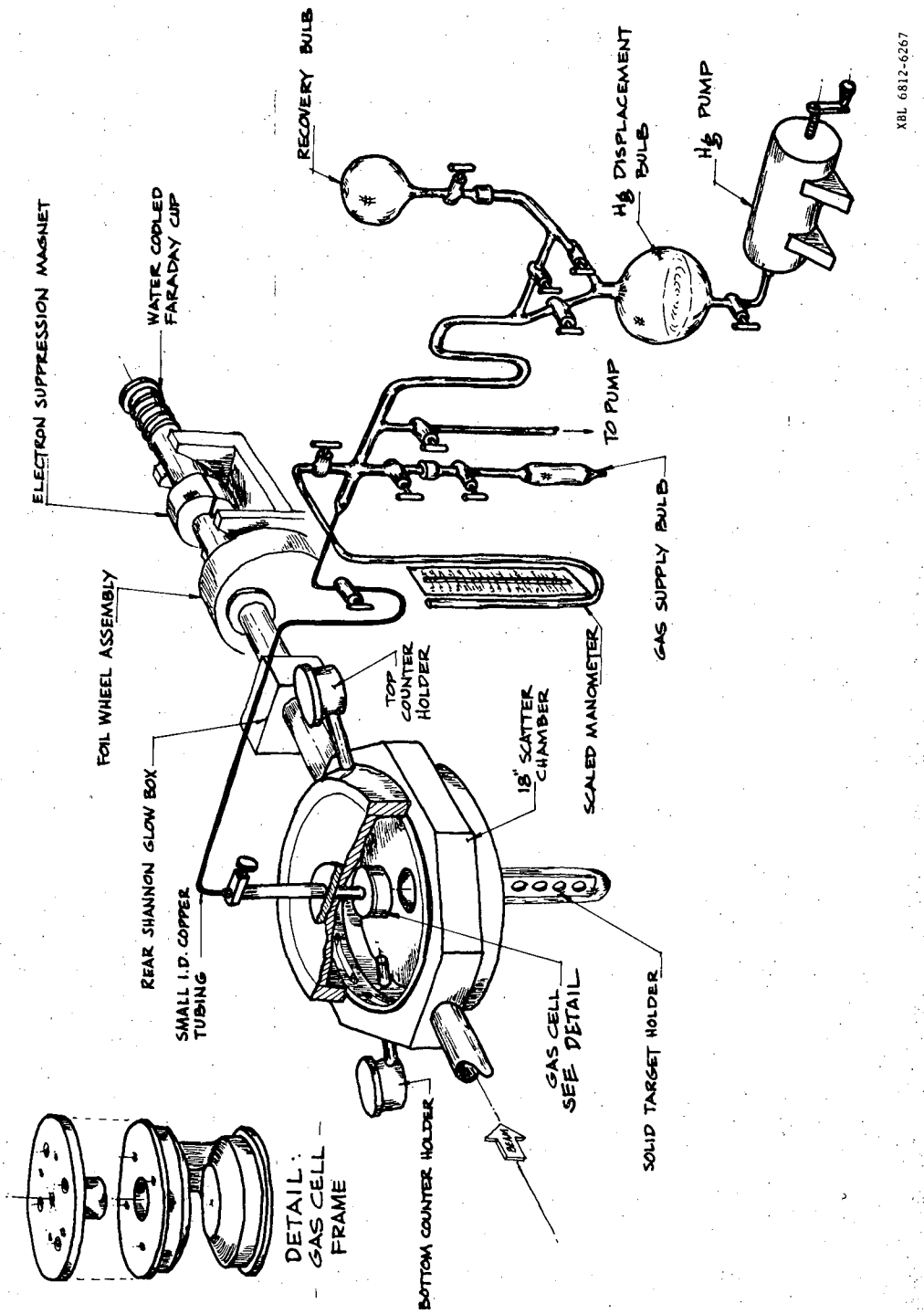
RECOVERY BULB
Hg DISPLACEMENT BULB
Hg PUMP
XBL 6812-6267
ELECTRON SUPPRESSION MAGNET
WATER COOLED FARADAY CUP
TO PUMP
FOIL WHEEL ASSEMBLY
TOP COUNTER HOLDER
GAS SUPPLY BULB
18" SCATTER CHAMBER
SCALED MANOMETER
REAR SHANNON GLOW BOX
SMALL I.D. COPPER TUBING
GAS CELL SEE DETAIL
SOLID TARGET HOLDER
BEAM
BOTTOM COUNTER HOLDER
DETAIL: GAS CELL - FRAME

Fig. 1.

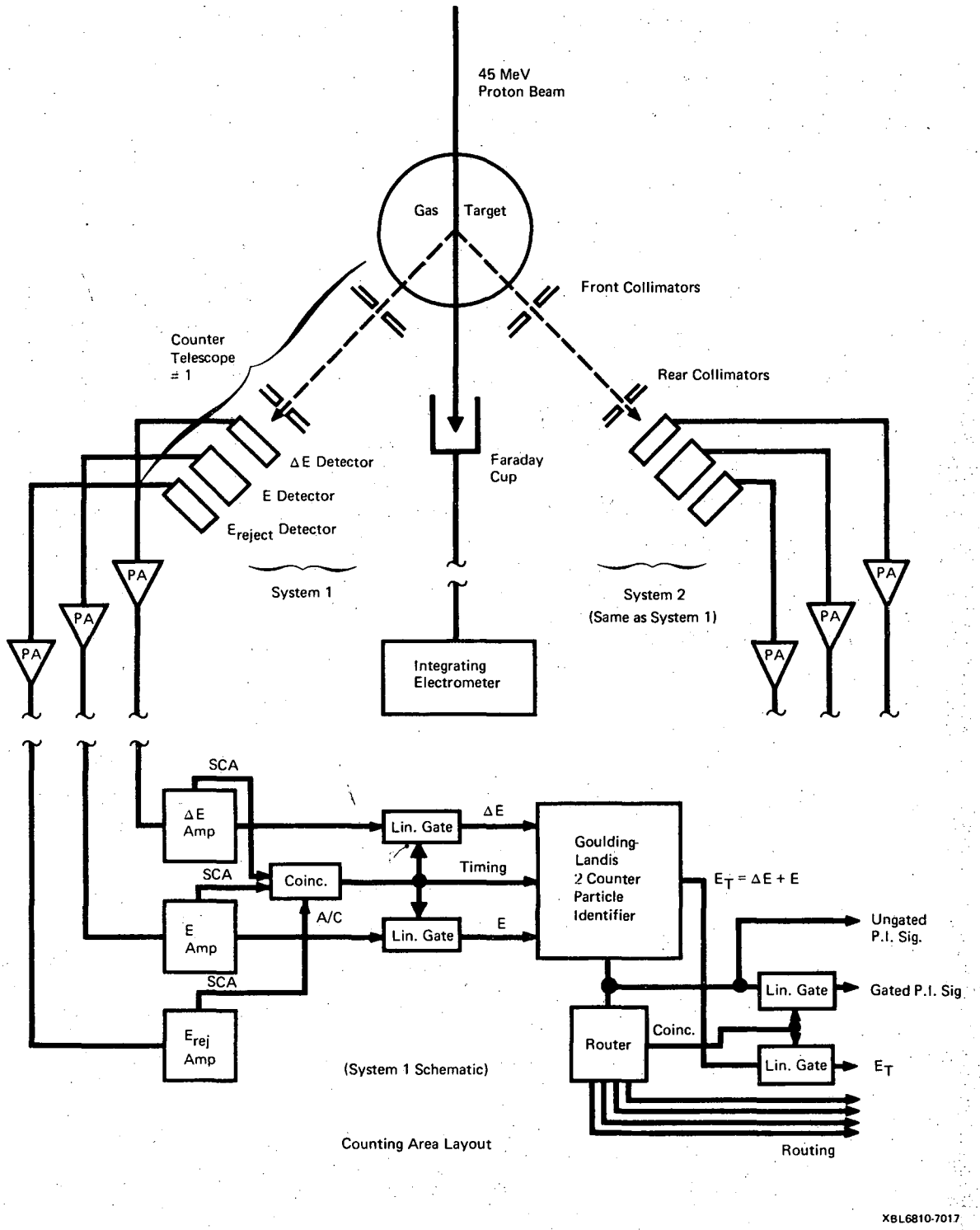
45 MeV
Proton Beam
Gas
Target
Front Collimators
Counter
Telescope
1
Rear Collimators
ΔE Detector
E Detector
E reject Detector
Faraday
Cup
System 1
System 2
(Same as System 1)
PA
Integrating
Electrometer
SCA
ΔE
Amp
Lin. Gate
ΔE
Goulding-
Landis
2 Counter
Particle
Identifier
SCA
Coinc.
Timing
E
Amp
A/C
Lin. Gate
E
SCA
E rej
Amp
(System 1 Schematic)
E T = ΔE + E
Ungated
P.I. Sig.
Lin. Gate
Gated P.I. Sig
Router
Coinc.
Lin. Gate
E T
Counting Area Layout
Routing
XBL6810-7017

Fig. 2.

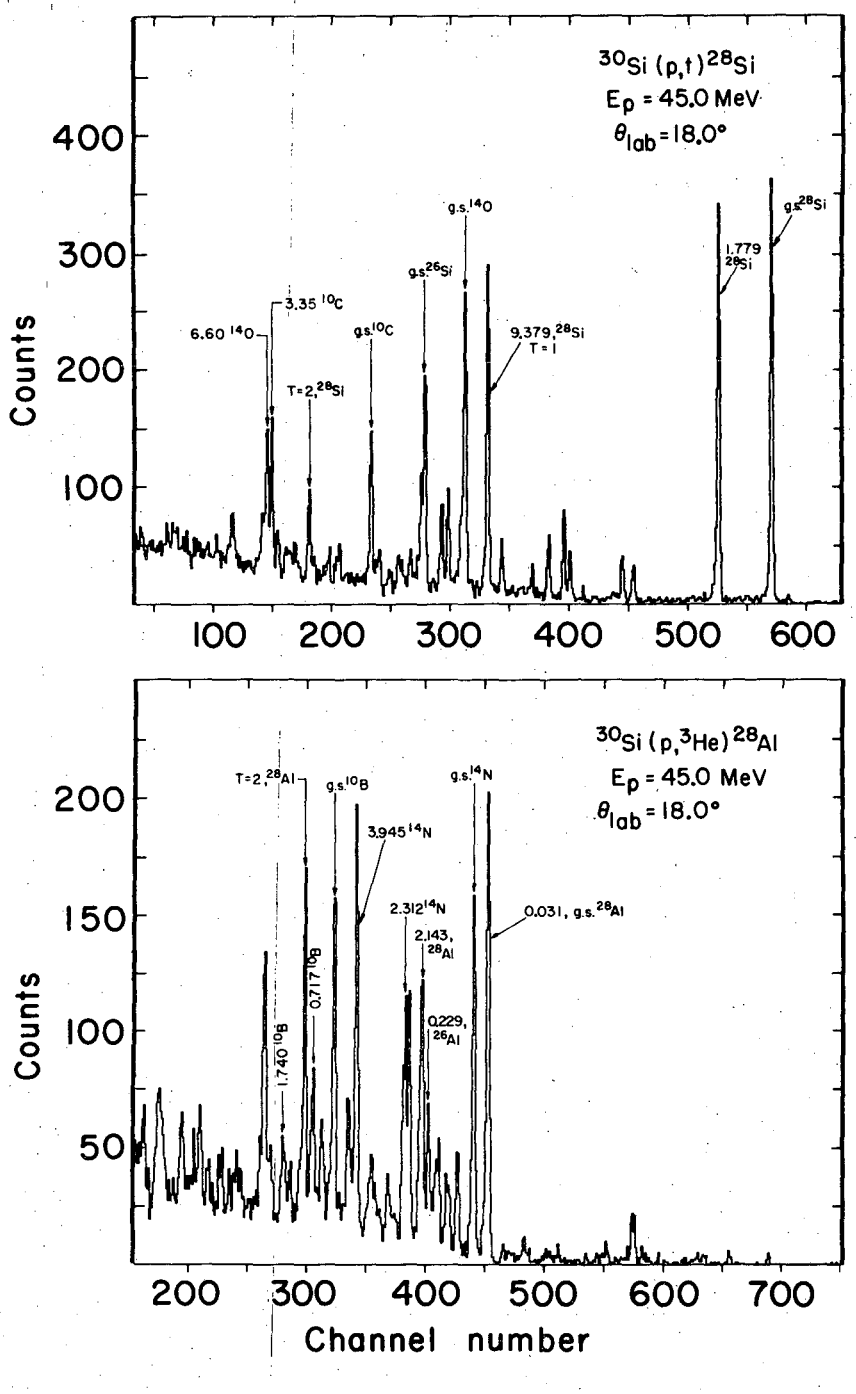
^{30}Si (p,t)^{28}Si
Ep = 45.0 MeV
θlab = 18.0°
g.s.^{14}O
g.s.^{28}Si
1.779 ^{29}Si
g.s.^{26}Si
3.35 ^{10}C
6.60 ^{14}O
g.s.^{10}C
9.379, ^{28}Si T=1
T=2, ^{28}Si
Counts
400
300
200
100
100 200 300 400 500 600
^{30}Si (p,^{3}He)^{28}Al
Ep = 45.0 MeV
θlab = 18.0°
T=2, ^{28}Al
g.s.^{10}B
g.s.^{14}N
3.945 ^{14}N
2.312 ^{14}N
2.143, ^{28}Al
0.031, g.s. ^{28}Al
0.717 ^{10}B
1.740 ^{10}B
0.229, ^{26}Al
Counts
200
150
100
50
200 300 400 500 600 700
Channel number
XBL6812-7508

Fig. 3.

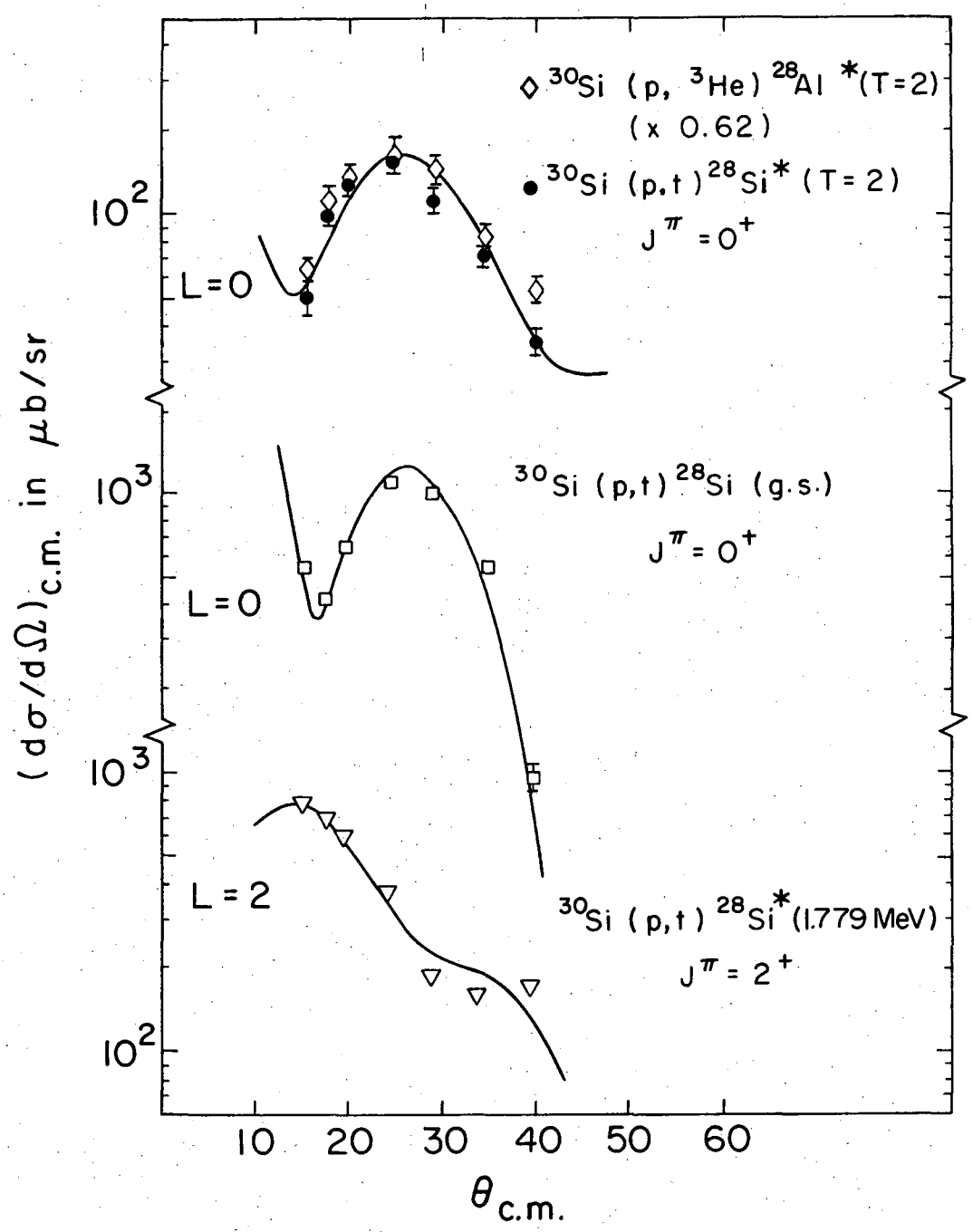

XBL697-3215

Fig. 4.

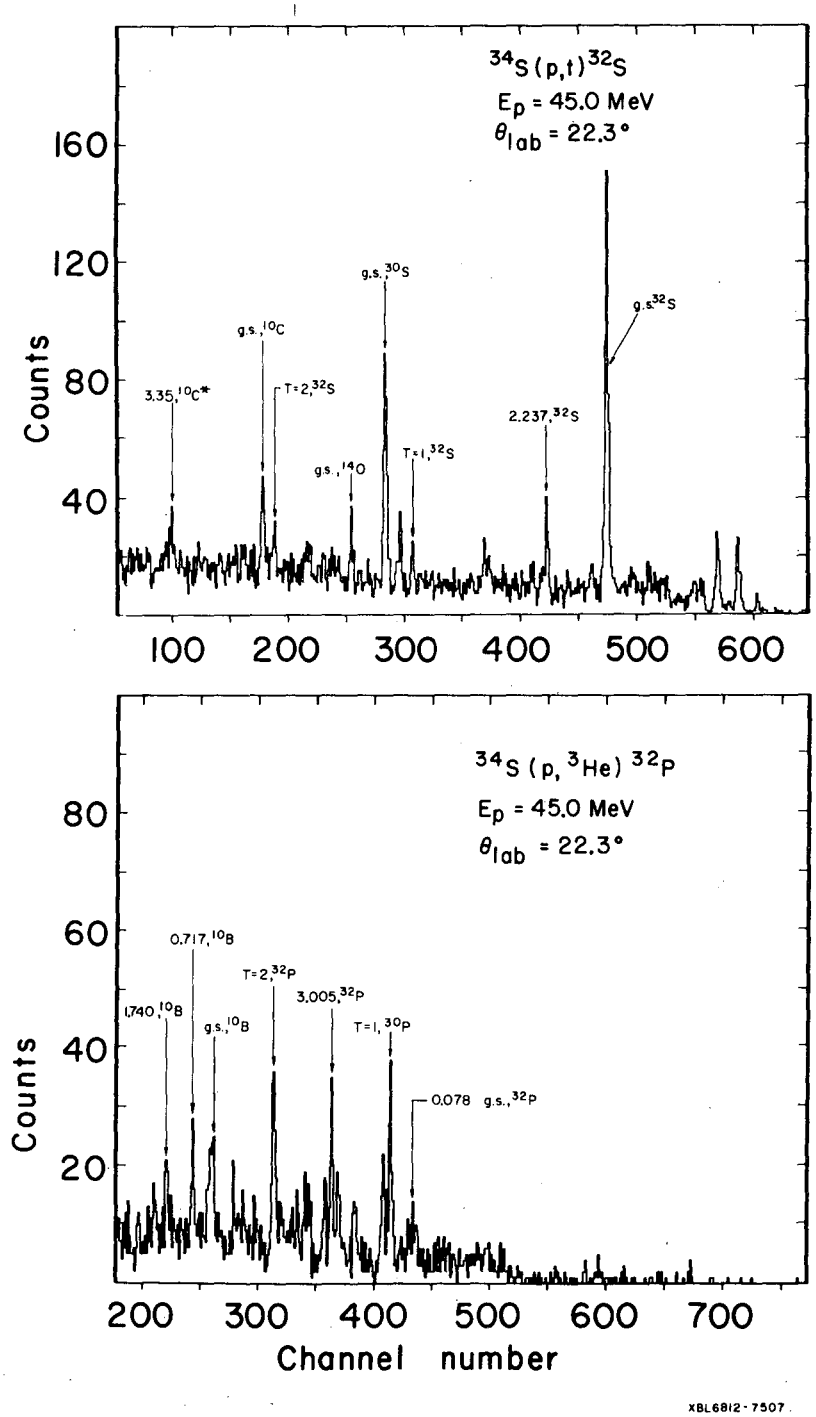
$^{34}S(p,t)^{32}S$
E_p = 45.0 MeV
θ_{lab} = 22.3°
Counts
160
120
80
40
3.35, $^{10}C^*$
g.s., ^{10}C
T=2, ^{32}S
g.s., ^{14}O
g.s., ^{30}S
T=1, ^{32}S
2.237, ^{32}S
g.s. ^{32}S
100
200
300
400
500
600
$^{34}S(p,^3He)^{32}P$
E_p = 45.0 MeV
θ_{lab} = 22.3°
Counts
80
60
40
20
0.717, ^{10}B
1.740, ^{10}B
g.s., ^{10}B
T=2, ^{32}P
3.005, ^{32}P
T=1, ^{30}P
0.078 g.s., ^{32}P
200
300
400
500
600
700
Channel number
XBL6812-7507

Fig. 5.

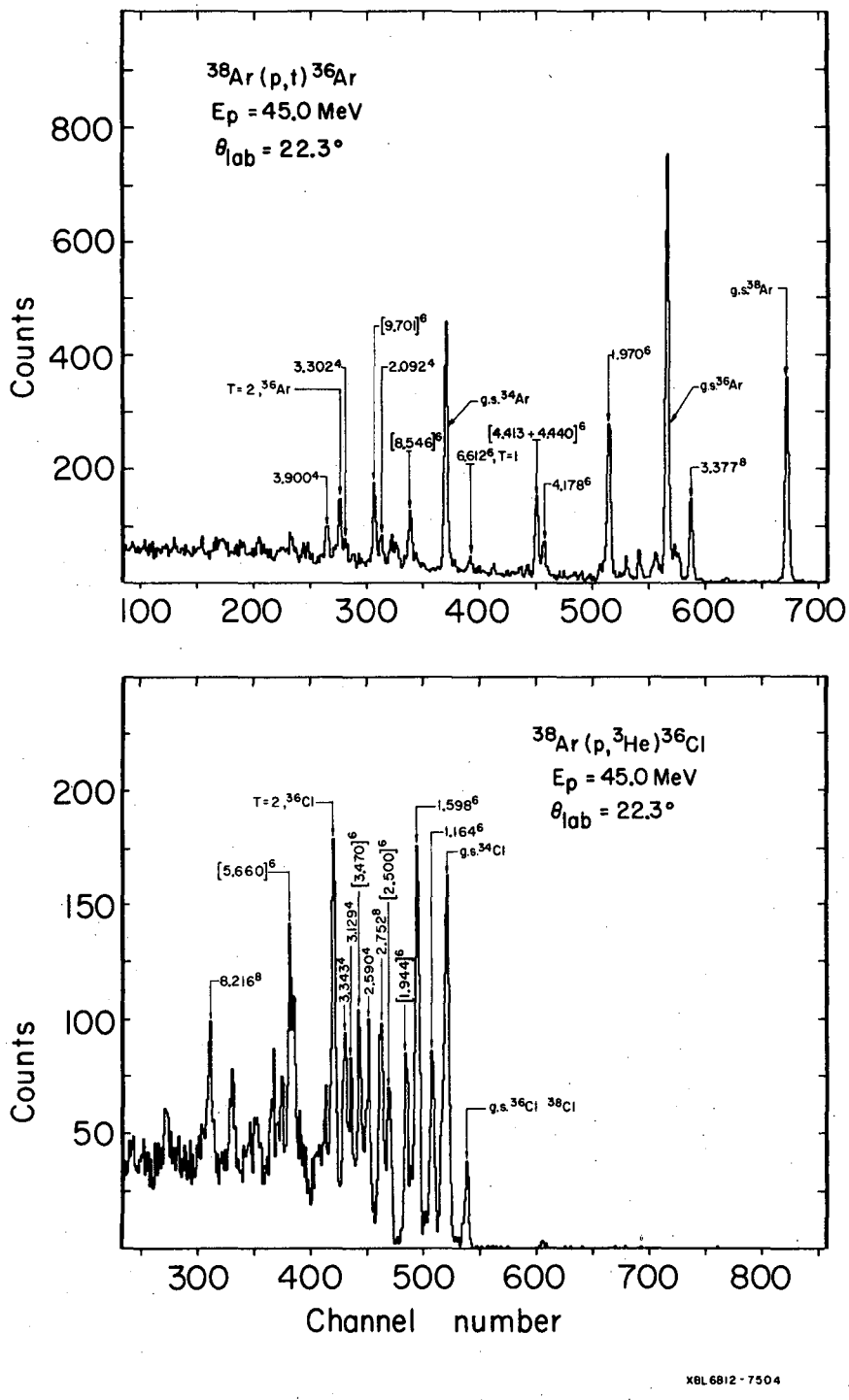
^{38}Ar (p,t) ^{36}Ar
Ep = 45.0 MeV
θ_{lab} = 22.3°
Counts
800
600
400
200
100 200 300 400 500 600 700
T=2, ^{36}Ar
3.302^{4}
3.900^{4}
[9.70]^{6}
2.092^{4}
g.s. ^{34}Ar
[8.546]^{6}
[4.413 + 4.440]^{6}
6.612^{6}, T=1
4.178^{6}
1.970^{6}
g.s. ^{38}Ar
g.s. ^{36}Ar
3.377^{8}
^{38}Ar (p, ^{3}He) ^{36}Cl
Ep = 45.0 MeV
θ_{lab} = 22.3°
Counts
200
150
100
50
300 400 500 600 700 800
Channel number
T=2, ^{36}Cl
[5.660]^{5}
8.216^{8}
3.343^{4}
3.129^{4}
[3.470]^{6}
2.590^{4}
2.752^{8}
[2.500]^{6}
[1.944]^{6}
1.598^{6}
1.164^{6}
g.s. ^{34}Cl
g.s. ^{36}Cl ^{38}Cl
X8L6812-7504

Fig. 6.

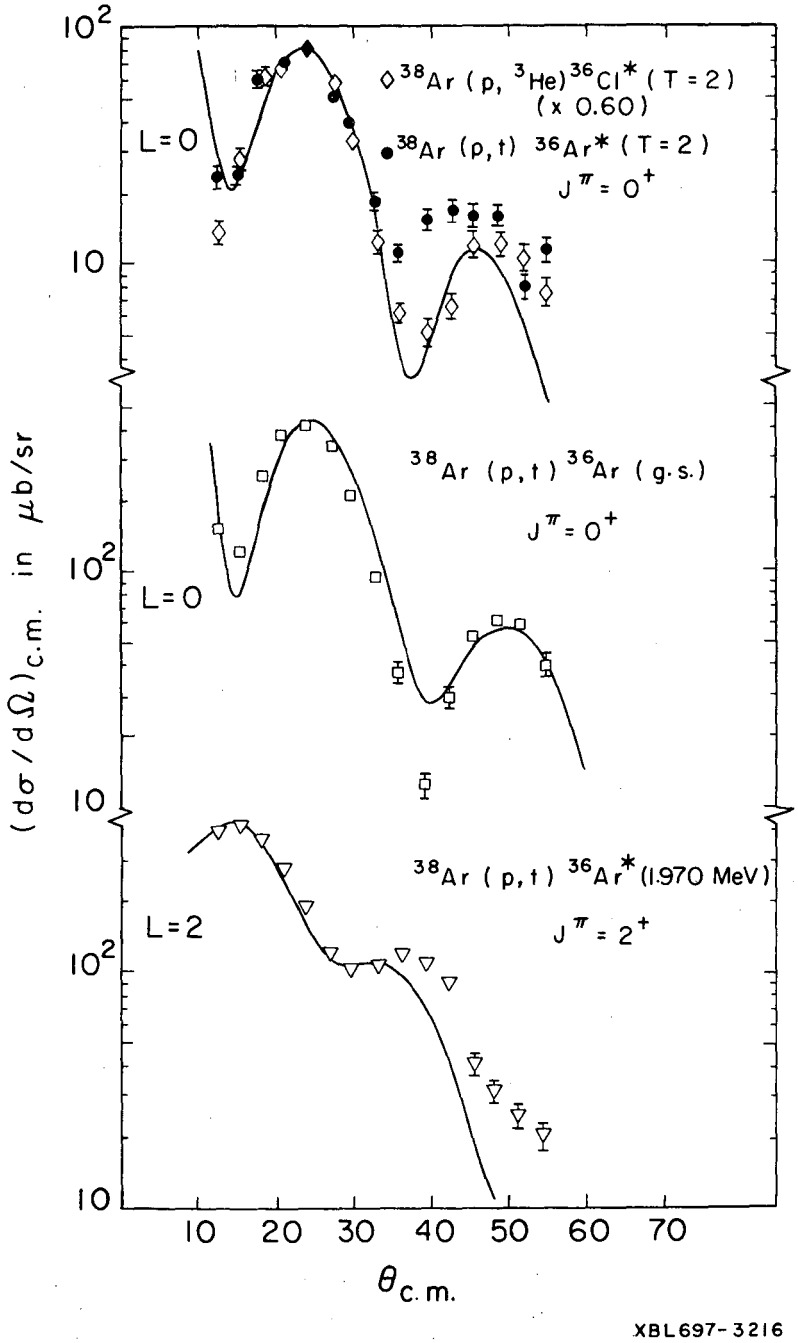

XBL697-3216

Fig. 7.

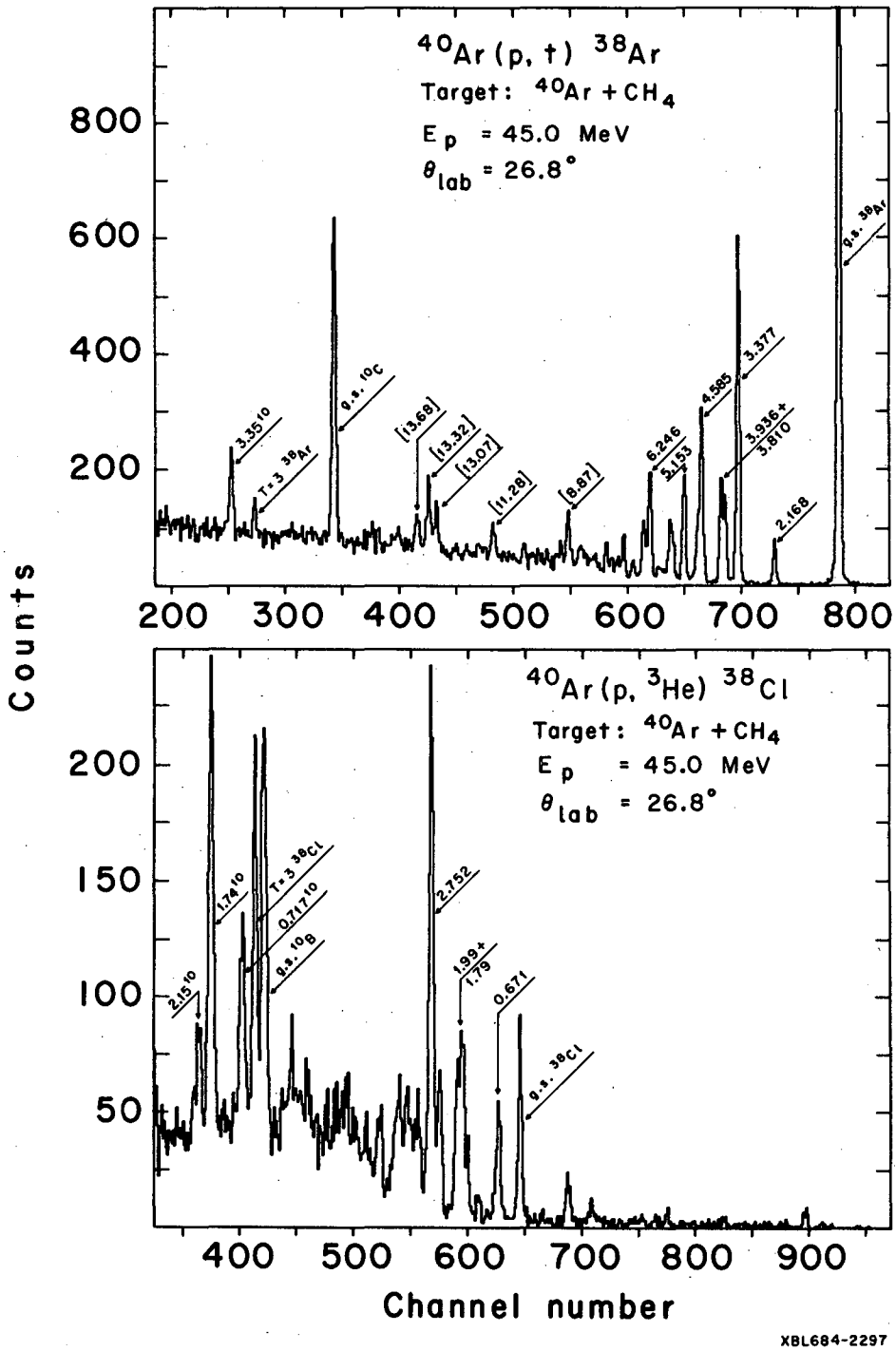
^{40}Ar (p, t) ^{38}Ar
Target: ^{40}Ar + CH$_4$
E$_p$ = 45.0 MeV
θ$_{lab}$ = 26.8°
g.s. ^{38}Ar
3.377
4.585
3.936+
3.810
6.246
3.153
2.168
3.35 ^{10}
T=3 ^{38}Ar
g.s. ^{10}C
[13.68]
[13.32]
[13.07]
[11.28]
[9.87]
^{40}Ar (p, ^{3}He) ^{38}Cl
Target: ^{40}Ar + CH$_4$
E$_p$ = 45.0 MeV
θ$_{lab}$ = 26.8°
2.15 ^{10}
1.74 ^{10}
T=3 ^{38}Cl
0.717 ^{10}
g.s. ^{10}B
2.752
1.99+
1.79
0.671
g.s. ^{38}Cl
Counts
Channel number
XBL684-2297

Fig. 8.

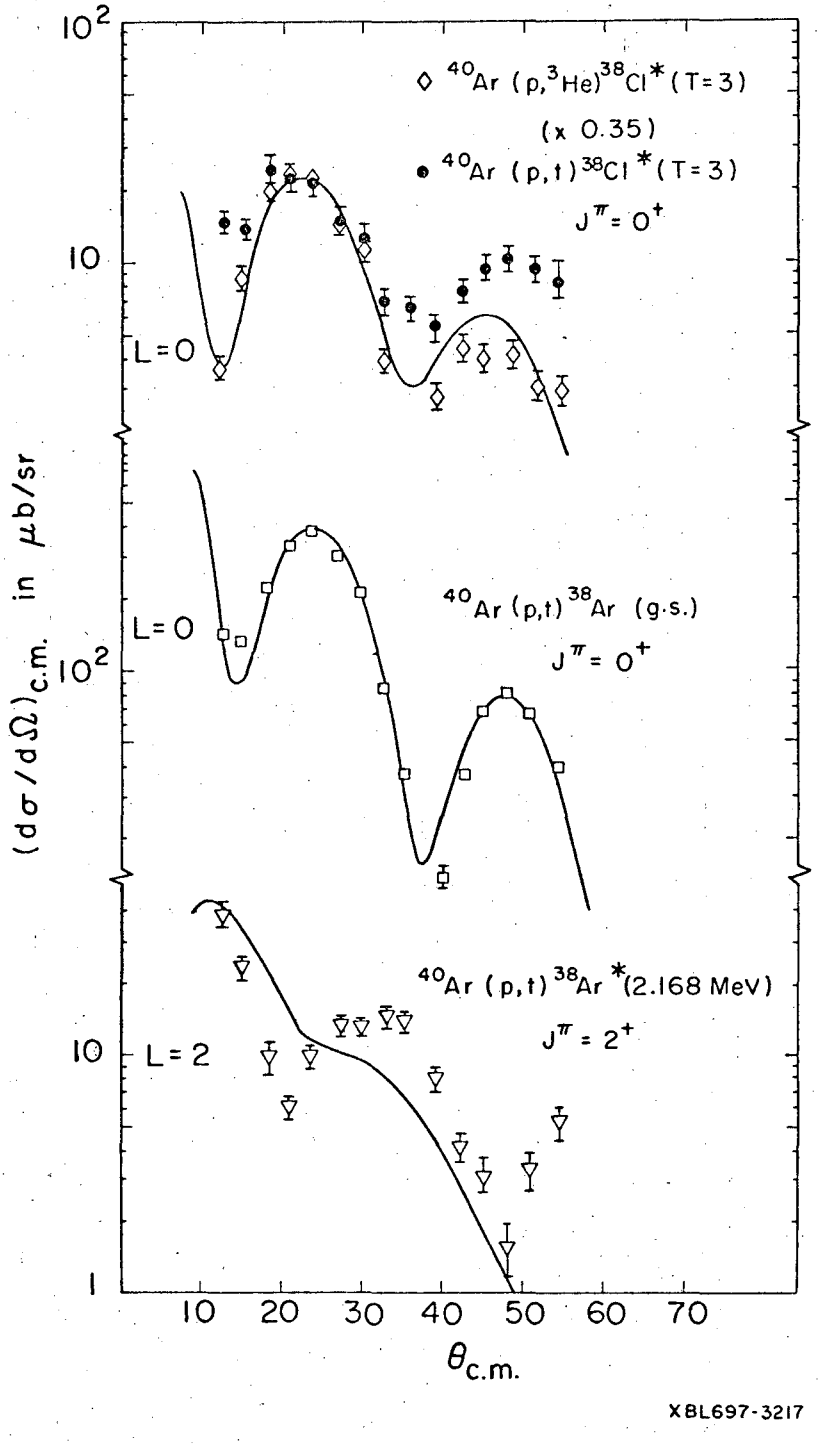
10^2
10
1
$(d\sigma/d\Omega)_{c.m.}$ in μb/sr
◇ ^{40}Ar (p,^{3}He)^{38}Cl* (T=3)
(x 0.35)
● ^{40}Ar (p,t)^{38}Cl* (T=3)
$J^\pi = 0^+$
L=0
^{40}Ar (p,t)^{38}Ar (g.s.)
$J^\pi = 0^+$
L=0
^{40}Ar (p,t)^{38}Ar* (2.168 MeV)
$J^\pi = 2^+$
L=2
10 20 30 40 50 60 70
$\theta_{c.m.}$
XBL697-3217

Fig. 9.

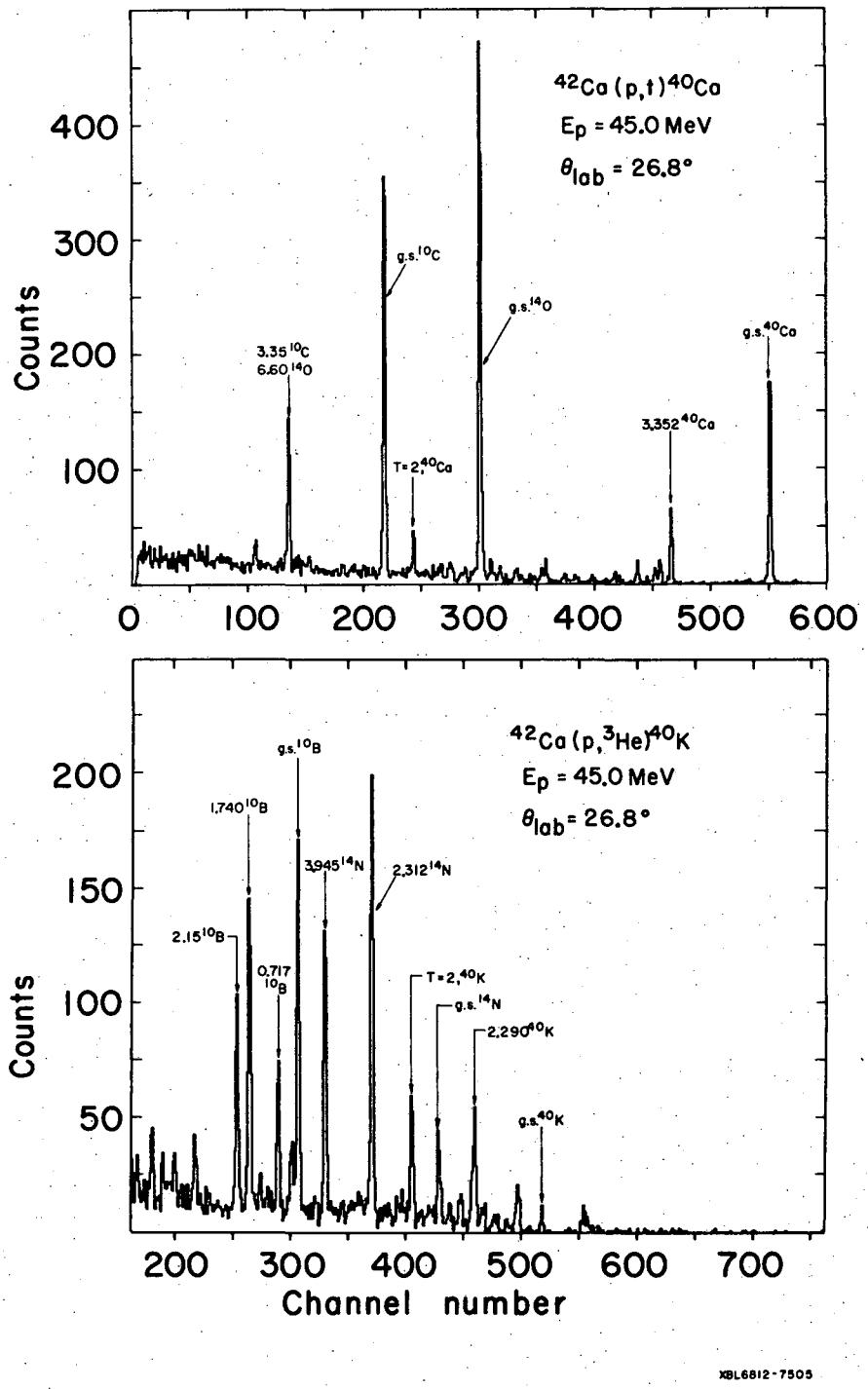
^{42}Ca (p,t)^{40}Ca
Ep = 45.0 MeV
θlab = 26.8°
g.s. ^{10}C
g.s. ^{14}O
g.s. ^{40}Ca
3.35 ^{10}C
6.60 ^{14}O
T=2, ^{40}Ca
3.352 ^{40}Ca
Counts
^{42}Ca (p, ^{3}He)^{40}K
Ep = 45.0 MeV
θlab = 26.8°
g.s. ^{10}B
1.740 ^{10}B
3.945 ^{14}N
2.312 ^{14}N
2.15 ^{10}B
0.717 ^{10}B
T=2, ^{40}K
g.s. ^{14}N
2.290 ^{40}K
g.s. ^{40}K
Counts
Channel number
XBL6812-7505

Fig. 10.

TECHNICAL INFORMATION DIVISION
LAWRENCE RADIATION LABORATORY
UNIVERSITY OF CALIFORNIA
BERKELEY, CALIFORNIA 94720